Social Interaction-induced Activation of RNA Splicing in the Amygdala of Microbiome-Deficient Mice

Roman M Stilling[1,2,*], Gerard M Moloney[1,2], Feargal J Ryan[1,3], Alan E Hoban[1,2], Thomaz Bastiaanssen[1], Fergus Shanahan[1], Gerard Clarke[1,4], Marcus J Claesson[1,3], Timothy G Dinan[1,4], John F. Cryan [1,2§]

[1]APC Microbiome Institute, University College Cork, Cork, Ireland
[2]Department of Anatomy and Neuroscience, University College Cork, Cork, Ireland
[3]Department of Microbiology, University College Cork, Cork, Ireland
[4]Department of Psychiatry and Neurobehavioural Science, University College Cork, Ireland
*present address: German Primate Center, Goettingen, Germany
[§]corresponding author

Abstract

Social behaviour is regulated by activity of host-associated microbiota across multiple species. However, the molecular mechanisms mediating this relationship remain elusive. We therefore determined the dynamic, stimulus-dependent transcriptional regulation of germ-free (GF) and GF mice colonised post weaning (exGF) in the amygdala, a brain region critically involved in regulating social interaction. In GF mice the dynamic response seen in controls was attenuated and replaced by a marked increase in expression of splicing factors and alternative exon usage in GF mice upon stimulation, which was even more pronounced in exGF mice. In conclusion, we demonstrate a molecular basis for how the host microbiome is crucial for a normal behavioural response during social interaction. Our data further suggest that social behaviour is correlated with the gene-expression response in the amygdala, established during neurodevelopment as a result of host-microbe interactions. Our findings may help toward understanding neurodevelopmental events leading to social behaviour dysregulation, such as those found in autism spectrum disorders (ASDs).

Introduction

The tight association that animals have with the trillions of microbes that colonise them is the result of a long evolutionary history. Although we only very recently started to understand the intimate relationship between microbes and host physiology, including brain function, it is now well accepted that host neurodevelopment, brain function and behaviour are regulated by presence and activity of the host-associated microbiota [1–7].

One of the most recurrent and evolutionary conserved behaviours observed to be influenced by the microbiota, both during a host's lifetime as well as on evolutionary time scales, is host social behaviour [8–24]. Importantly, a growing body of data in healthy volunteers and patient populations is emerging indicating microbial influences also translate to human emotional behaviours [25] and have been suggested to play a role in neurodevelopmental disorders such as autism spectrum disorders (ASDs) [22,26–29] and schizophrenia [30]. Just very recently, it was shown in two independent mouse models of autism that the microbiota is necessary for expression of autistic-like symptoms in these models [31,32]. It is, however, still largely unclear how and where the microbiota influence brain function and which mechanisms mediate changes in behaviour.

While the amygdala is critically involved in anxiety and fear-related behaviours and memory, it is also a well-established key emotional brain centre for evaluating and responding to social stimuli in humans and other mammals [33–39]. As such, neuropsychiatric disorders characterised by social deficits (including autism spectrum and anxiety disorders) are associated with structural and functional changes in the amygdala [40–43]. Evidence for a role of the microbiota in regulating amygdala function is emerging [25,44–47] but this has been largely descriptive.

Germ-free (GF) mice, lacking microbial colonisation throughout development, are a well-established and essential tool spearheading the characterisation of microbiota-host

interactions in regulating development and physiological and behavioural parameters in the host [11,26,48–55]. By colonising GF mice at a weaning age (exGF), developmental effects can be distinguished from dynamic, reversible effects of a functional microbiota. Previous studies focussed on the ability of post-weaning colonisation of formerly GF rodents to reverse behavioural deficits have produced mixed results with some phenotypes being reversible while others seemed to be developmentally programmed (see [56] for review). Thus, the mechanistic underpinnings of behavioural changes in GF mice and how they are controlled by early colonisation during development are still elusive.

We here provide evidence that the microbiota is a critical regulator of social interaction-induced gene expression in the amygdala. Using an unbiased, genome-wide approach to determine gene expression in the amygdala by paired-end, stranded, ribodepleted RNA-sequencing together with a comprehensive downstream analysis pipeline, we studied alterations in the amygdala transcriptome in response to a social interaction stimulus. We find a unique transcriptional response in GF mice that involves upregulation of the splicing machinery, which is able to partially compensate for impairments in neuronal plasticity signalling during social interaction in these animals.

Results

Germ-free mice display impaired sociability behaviour with high inter-individual variability

Mice lacking any interaction with microorganisms throughout development have a range of behavioural phenotypes [55], including memory impairments and altered anxiety behaviour [44,57].

Here, we subjected conventional mice (CON-SI), germ-free mice (GF-SI), and germ-free mice colonized after weaning (exGF-SI) to a social stimulus (the three-chamber social interaction test (3CSIT), based on [58]) and measured the time during which the test mice interacted with a conventional conspecific male mouse or a non-social object (**Fig. 1A**, experimental design and workflow). As previously reported [11,59], on average the group of GF-SI mice showed significantly decreased interaction with a conspecific compared with controls and colonized animals, while interaction with the non-social object was similar among the three groups (**Fig. 1B-C**). Notably, we found high inter-individual variability in the GF-SI group for the time interacting with the conspecific, ranging from approximately control levels (>300 s) to as little as 60 s (**Fig. 1B**). However, the distribution passed the D'Agostino & Pearson omnibus normality test, the Shapiro-Wilk normality test and the KS normality test, all at alpha=0.05. Time spent with the non-social object was similarly variable in all three groups (**Fig. 1C**).

Social interaction induces highly distinct gene expression patterns in the amygdala of germ-free mice

Since we have previously shown that social interactions in the mouse 3CSIT behavioural paradigm reliably activates stimulus-dependent genes expression in the amygdala [45], we hypothesised that we would observe changes in gene expression in this brain region as a function of colonisation status and, especially, social experience. Thus we sought to identify potential molecular pathways involved in mediating microbiome-to-brain signalling by systematically comparing gene expression patterns in the amygdala of mice that were exposed to social environmental stimulation (social interaction, SI) mice. To this end, we retrieved RNA from naïve animals and 1 hour after the social experience for CON, GF and exGF animals and performed a highly comprehensive type of RNA-sequencing, using paired-end RNA libraries that retains information on which DNA strand was transcribed and includes also non-polyadenylated RNA species. This way our analysis incorporated gene expression

changes at baseline and in response to stimulus-induced transcription of both, mRNAs and long non-coding RNAs (lncRNAs) that lack a poly-A tail.

In a first step, we performed analysis of differential gene expression on all meaningful pairwise comparisons (**Table 1**). When comparing the number of differentially expressed genes (DEGs, both up- and downregulated) between naïve animals of different colonisation status, we find the highest number of DEGs in the CON-GF comparison (**Fig. 2A, Supplementary File 1**), as we have previously reported in an independent study [45]. Interestingly, when comparing naïve vs. stimulated animals the response in terms of number of DEGs was strongest in GF animals by far, providing evidence for the amygdalar transcriptomes to diverge between the three groups upon environmental stimulation by social interaction. Transcriptional divergence driven by neuronal activity is further supported by the number of DEGs when comparing the SI groups among each other, as these numbers are substantially (4 - 9 times) higher than DEG numbers for naïve comparisons (**Fig. 2A**). Increasing stringency of the analysis (log2(fold-change) > |±0.5|) had little relative effect on these results (**Fig. S1A**).

Table 1: Meaningful pairwise comparisons for gene expression changes (9 unique comparisons).

Group	Environmental stimulation	Compared to
CON (n=4)	Naïve (n=4, representing 8 animals, per group)	GF, exGF, CON-SI
GF (n=4)		CON, exGF, GF-SI
exGF (n=4)		CON, GF, exGF-SI
CON-SI (n=8)	social interaction (SI)	CON, GF-SI, exGF-SI
GF-SI (n=12)		GF, CON-SI, exGF-SI
exGF-SI (n=8)		exGF, CON-SI, GF-SI

Next we looked for overlapping DEGs between pairwise comparisons. Because meaningful Venn diagrams are limited to four or five comparisons, to identify groups of genes that are regulated in multiple comparisons, we plotted the presence or absence for each of the 4522 non-redundant genes found in any of the comparisons (**Fig. 2B**). As expected, there were

multiple overlapping clusters between SI comparisons, demonstrating a core cluster of genes that are induced 1 hour after social novelty, independent of colonisation status. However, multiple clusters of genes showed differential regulation only in a particular group, suggesting differences in the transcriptomic response of the individual groups. We identified a cluster of genes that was differentially regulated in both GF naïve animals and upon social interaction stimulation in conventional animals (**Fig. 2C**). This overlap was highly significant and made up large proportions of all genes up- or downregulated in naive GF animals compared to CON controls (38% and 26%, respectively). This cluster was not differentially regulated in GF animals upon stimulation by social interaction (**Fig. 2D**). In fact, there was a counter directional overlap (e.g. genes upregulated in CON vs. GF but downregulated in GF upon stimulation) Together, these data suggest that several genes typically induced in the amygdala of conventional controls upon social interaction are already elevated in GF mice, pointing towards amygdalar hyperactivity in these animals [45].

To identify pathways and biological functions that are induced in the amygdala by social interaction under the different colonisation conditions, we next analysed the dataset for functional enrichment. To this end, we tested upregulated genes for each group for enrichment of biological functions using the gene ontology (GO) database and compared resulting p-values (**Fig. 2E, Supplementary File 2**). We found a wide-range of biological functions to be enriched in the three conditions. While overall the groups differed substantially, we identified one cluster that showed good agreement between comparisons. For all three groups significant enrichment was found for processes such as protein modification and folding as well as regulation of gene expression. This is in good agreement with the fact that there is a core cluster of genes overlapping (see **Fig. 2B**). However, large differences were also seen in processes that are associated with intracellular signalling such as protein phosphorylation and dephosphorylation, which was enriched in the CON-SI comparison, but not in GF-SI or exGF-SI. The second striking difference was dramatic enrichment of processes associated with RNA splicing, most prominently in the GF-SI but also exGF-SI group (**Fig. 2E, Supplementary File 3**). Using gene-set enrichment analysis

(GSEA), which does not rely on cut-offs for p-value or fold-change, we find similar differences in functional enrichment (Supplementary File 2).

We also analysed the dataset for enrichment of genes associated with specific cellular pathways using the KEGG pathways database. As expected, in the CON-SI group the MAP kinase (MAPK) signalling pathway was the dominant pathway enriched due to social interaction treatment (**Fig. 3A, Supplementary File 2**). This pathway, which is well established to be induced upon neuronal activity, was also enriched in GF-SI and exGI-SI groups, albeit to a much lesser degree. In fact, under more stringent analysis parameters enrichment failed to reach significance in these groups (**Fig. S1A**). For the GF-SI group we found a highly significant enrichment of genes associated with the spliceosome that was also significantly enriched, to a lesser extent, in the exGF-SI group and almost completely absent from the CON-SI group (**Fig 3A**). To elucidate the differences in gene regulation in response to social interaction between CON and GF mice we analysed genes exclusively induced in either of the groups for further functional enrichment. In line with GO Term and KEGG pathway analysis we found that DEGs exclusively upregulated in CON-SI mice, were highly enriched in genes involved in intracellular signalling, especially the MAPK pathway, while DEGs exclusively upregulated in GF-SI mice were strongly enriched in genes associated with RNA processing, i.e. splicing (**Fig 3B, Supplementary File 2**). The core of genes that are induced independent of colonisation status is characterised by enrichment of genes involved in protein folding and, to a lesser degree, both, spliceosome and MAPK signalling pathway. Genes falling into these two KEGG categories made up relatively large proportions of all DEGs in the CON-SI or the GF-SI group, respectively **(Fig 3C, Supplementary File 2**). Genes associated with the GO Term “RNA processing” made up 4.4% of all DEGs in the GF-SI group (111/2510), which represents 15% of all mouse genes in this category (111/741). Comparing response-induced fold changes of these 111 genes between colonisation statuses, further highlighted that expression of this group of genes is highly distinctive in GF-SI animals (**Fig. 3D**). This unique pattern was also evident when we plotted a comparison of these genes, where the individual gene identity was maintained across groups and where

mean expression values for the remaining 630, not statistically significant mouse genes in the "RNA processing" GO category for each group were included (**Fig. S1B**).

Stimulus-induced upregulation of a number of well-established immediate early genes, that show rapid and reproducible upregulation in response to neuronal activity, including activity induced by environmental novelty in the hippocampus, was also seen in the amygdala of conventional animals after social interaction (**Fig. S1C**). In line with reduced activation of the MAPK pathway in GF-SI mice, we find several of these genes, including *Egr3*, *Fos*, and *Ier5* not to be upregulated in this group, possibly due to elevated expression levels at baseline (**Supplementary File 1**).

Together these data suggest that GF animals show a unique response signature toward environmental stimulation by social interaction. The transcriptional response is characterised by a marked upregulation of the genes involved in RNA processing and the splicing machinery, accompanied by an arrested upregulation of typical response genes, especially in those involved in MAPK signalling. Analysis of differential gene expression between naïve GF animals and controls also revealed that this lack of induction may be due to upregulation of several genes involved in these processes already at baseline. All analyses on GF animals colonised with a conventional microbiota at weaning (exGF) presented so far show results with features of both, CON and GF groups.

Social interaction leads to a strong increase in alternative splicing in GF and exGF animals

Since "RNA processing" and spliceosome-associated pathways were highly enriched in the amygdala of GF animals and also exGF animals, we next analysed our dataset for functional consequences of this upregulation by searching for alternative splicing events, i.e. differentials spliced genes (DSGs). Under naïve conditions alternative splicing was highest when comparing CON and GF animals (**Fig. 4A, Supplementary File 4**). These genes were highly enriched in several functional categories involved in neuronal function, such as long-term potentiation (p_{adj}=2.3e-6) and synaptic transmission (p_{adj}=1.2e-10) (**Supplementary File**

206 **5**). Similar enrichment, although to a lesser degree was found when comparing GF and exGF
207 animals, while no significant functional enrichment was found for the relatively few DSGs in
208 the CON vs. exGF comparison. High congruence between alternative splicing between CON
209 and exGF mice was also evident from the high degree of overlap between DSGs that
210 distinguished both groups from the GF group (**Fig. 4B**). Together these data are in
211 agreement with phenotypic similarities between CON and exGF animals, i.e. reversibility of
212 the GF phenotype by colonisation at weaning.

213 In line with diverging transcriptomes between groups due to differential gene expression after
214 stimulation by social novelty, the transcriptional landscapes changed substantially as a result
215 of alternative splicing. While conventionally colonised controls exposed to social interaction
216 showed comparatively little alternative exon usage, we found a dramatically increased
217 number of DSGs in the GF-SI group, and noticed an even higher number of SI-induced
218 DSGs in exGF animals. This was surprising since enrichment of splicing associated genes
219 among DEGs was highest in the GF-SI comparison, albeit significantly present also in the
220 exGF-SI group.

221 As with the previous finding for DEGs, DSGs of the three comparisons also shared a 'core'
222 set of genes that were alternatively spliced in response to social interaction, independent of
223 colonisation status (**Fig. 4C**). This core was slightly enriched in genes associated with
224 functional categories that are involved in neuronal function such as long-term potentiation
225 (1.5e-02) and synaptic transmission (1.9e-4). In fact, the high degree of overlap between all
226 three groups together with the high number of DSGs in GF-SI and exGF-SI groups suggests
227 that, in addition to the conventional response, these two groups show supplementary cellular
228 responses towards activation of the amygdala by social interaction. Interestingly, this
229 additional response is even more pronounced in the exGF-SI group and is characterised by a
230 high number of DSGs highly enriched in genes involved in mainly four principal functional
231 categories: splicing/RNA processing, protein turnover, neuronal functions, and intracellular
232 signalling pathways (**Fig. 4D**, **Supplementary File 6**). The fact that a highly enriched

proportion of the alternatively spliced genes themselves were also members of the splicing machinery suggests a self-regulating mechanism of gene expression in these two groups.

Behavioural performance correlates with expression of RNA processing genes in GF mice

Given the high behavioural variability in active social interaction time specifically in the GF-SI group together with the divergence of the transcriptional landscape in the amygdala one hour after exposure, we hypothesised that gene expression may be correlated with behavioural performance in individual mice. To test this hypothesis, we ranked all expressed genes in our dataset by correlation (Pearson correlation coefficient) between expression level and time spent in active social interaction (**Supplementary File 7**). In order to identify functions that are associated with positively or negatively correlated genes we used the *Gene Set Enrichment Analysis* (GSEA) algorithm that assigns one or multiple functions to each gene in the list based on the GO Term or KEGG Pathway databases [60]. The algorithm then calculates an enrichment score for each function based on the rank of genes associated with this function (**Fig. 5 B,C**). Excitingly, genes whose expression was positively correlated with social interaction time were significantly associated with splicing, along with protein turnover (**Fig. 5B-D**). There was no significant gene set enrichment for negative correlations between sociability behaviour and gene expression. These data suggest direct involvement of splicing and protein turnover pathways in the amygdala with behavioural performance. This result was confirmed, when we compared gene expression between comparing the six germ-free animals with the highest social behaviour performance (GF-SI^{high}) with those six animals with lowest social behaviour performance (GF-SI^{low}). We found three genes that were significantly higher expressed in GF-SI^{high} animals, namely *DnaJb6* (encoding a brain-enriched heat-shock family protein with chaperone function), *Cribp* (encoding a stimulus-inducible, brain-enriched, nuclear RNA-binding protein involved in mRNA stabilization), and *D030028A08Rik* (a long-noncoding RNA with yet unknown function). Also these three genes show a statistically significant correlation with behavioural performance in the GF-SI group (**Fig 5E**).

Discussion

The amygdala is a key node in the emotional processing network, responsible for processing social stimuli and fear-related cues [33–39,61]. A rapidly developing literature increasingly implicates the microbiome in host brain function and behaviour, especially in these emotion processing networks [9,46,50,51,53,62–64]. Social behaviour appears to be among the behaviours most intimately connected to a function microbiome [8,11,13,16,23,24,26,59,65,66]. However, the mechanistic underpinnings of this influence are only beginning to be resolved. Here we show, for what is to our knowledge the first time, that absence of the microbiome results in dysregulation of unique transcriptional-response pathways in the amygdala.

In line with previous reports, we show that microbes are necessary for development of appropriate sociability behaviour [8,11,59]. In agreement with these studies we show reduced sociability behaviour of GF mice in the three-chamber social interaction task, rescued by post-weaning colonisation with a conventional microbiome. However, we do not observe a lack of preference of the conspecific mouse over an inanimate novel object in GF mice. Interestingly, while on average the group of GF mice spent significantly less time interacting with a conspecific than conventionally raised animals, some individual mice of this group performed at control level. This finding suggests, that the underlying networks controlling sociability behaviour are subject to a dynamic regulation, possibly associated with differences in intracellular and extracellular neuronal signalling pathways due to subtle differences accumulating during individual development. However, the fact that exGF mice, colonised with a conventional microbiota at weaning age, spent an intermediate amount of time in social interaction with more control-like variability within the group, argues that this development is highly susceptible to influence by symbiotic signals from the microbiota. Also in several analyses of gene expression regulation in response to social interaction exGF mice resemble an intermediate phenotype, bearing features of both CON and GF mice. As such, exGF mice show high enrichment of genes involved in “regulation of gene expression”

289 (most prominently enriched among CON-SI upregulated genes) as well as “RNA processing”
290 (most prominently enriched among GF-SI upregulated genes). This intermediate gene
291 expression phenotype is also evident from the visualized functional enrichment using colour-
292 coded functional GO-Terms (**Fig. 2E**).
293
294 To characterize real transcriptome-wide changes in gene expression, in this study we used
295 stranded, ribodepleted as opposed to poly-A enriched libraries for RNA-sequencing. In result,
296 we describe dynamic regulation of several previously undescribed pathways in response to
297 environmental stimulation. As such, we see regulation of RNA-processing non-coding RNAs,
298 several of which are found in subnuclear Cajal bodies, that are particularly prominent in
299 neurons - especially, when transcriptionally active - and are crucially involved in splicing
300 regulation [67,68]. Our RNA-seq experiment thus offers exclusive and comprehensive insight
301 into gene regulation in response to a social stimulus in the amygdala. Interestingly, induction
302 of gene expression in this brain region shows similarities with the hippocampal transcriptional
303 response to environmental novelty [69]. This overlap is very likely due to a ubiquitous, though
304 highly specific transcriptional response in neurons towards neuronal activity, which includes
305 induction of several well established immediate early genes such as *Fos* or *Arc*, the MAP-K
306 pathway, and neurotrophic signalling via *Bdnf*. Moreover, we find upregulation of
307 complement components, which have lately been established to be necessary for synaptic
308 rearrangements and plasticity upon neuronal activity [70–72]. Interestingly, innate immune
309 system genes together with neuronal activity-dependent genes have recently been shown to
310 be dysregulated in autism [73]. Induction of complement genes upon social interaction was
311 not seen in GF mice, possibly due to upregulation of *C1q* already under naïve conditions as
312 compared to CON mice. Indeed, we find that a highly significant share of genes upregulated
313 upon social interaction stimulation in CON mice is already upregulated in naïve GF mice. In
314 perfect agreement with previous reports [44,45], this finding suggests baseline hyperactivity
315 of neurons in the amygdala in GF mice. Together, these findings confirm that the expected
316 response of the control group serves as a positive control and provide internal validation that

317 the methodology of this study is able to detect relevant changes in transcriptional regulation
318 between groups.
319
320 Our data further shows that altered splicing activity is a normal process in neurons of the
321 amygdala in response to social interaction in conventionally raised mice. Indeed, it is now
322 well established, that neuronal activity induces alternative splicing patterns [74–77], a
323 dysfunction of which has been associated with changes seen in autism and autistic-like
324 behaviour in mice [78]. Surprisingly, the regulation of genes involved in splicing, including
325 Cajal body-associated genes, as well as alternative splicing activity is extremely exaggerated
326 in GF mice, which possibly reflects a compensatory mechanism for already elevated activity-
327 induced signalling at baseline. The finding that increased splicing activity is even more
328 amplified in exGF mice, which display a largely normalized behavioural response, together
329 with a positive correlation between expression of splicing-associated genes and behavioural
330 performance suggests that in fact upregulation of the splicing machinery supports an
331 adequate amygdalar response towards a social interaction environmental stimulus. In fact,
332 previous research shows that post-weaning colonization (exGF) does not rescue
333 impairments in social cognition, seen in GF mice [11]. This is likely a reflection of an
334 incomplete rescue of the molecular underpinnings of social behaviour investigated here.
335 Although beyond the scope of the current study and technically challenging future
336 investigations should focus on untangling the network and pathways that drive the observed
337 RNA processing changes and derive molecular consequences from altered mRNA / protein
338 amino acid sequences.
339
340 In summary, our data is fully congruent with and offers a molecular basis for previous data on
341 alterations in social cognition [11], amygdala volume and dendrite complexity [46], and
342 increased transcription of activity-associated gene expression in the amygdala [44,45] in
343 microbiome-deficient mice. We here show for what is to our knowledge the first time that the
344 microbiota is necessary for regulation of core biological processes on the molecular and

cellular level in the brain, which makes a strong case for a causal involvement of the microbiota in the molecular mechanisms leading to the observed impairments in sociability behaviour and the aetiology of neurodevelopmental diseases, which opens the possibility for new therapeutic strategies.

Materials and Methods

Animals

Male F_1-generation offspring from germ-free (GF) and conventionally-raised (CON) Swiss Webster breeding pairs previously obtained from Taconic (Germantown, New York, USA) were used in all experiments as previously described [11,45,50,79]. GF mice were housed in groups of two-four per cage in flexible-film gnotobiotic isolators at a 12-hour light/dark cycle. Ex-germ-free (exGF) mice were removed from the GF unit after weaning on postnatal day p21, and housed on CON-used bedding next to CON mice in the standard animal unit to allow colonization of microbes present in the facility environment. CON mice were similarly housed two–five per cage under controlled conditions (temperature 20–21 °C, 55–60% humidity) on the same 12 h light/dark cycle. All groups received the same autoclaved, pelleted diet (Special Diet Services, product code 801010). Age at tissue extraction for all groups and experiments was 10 weeks.

3-chamber social interaction test (3CSIT)

The 3CSIT was performed as described previously [11,45]. In brief, mice were habituated to the test room for half an hour and then habituated to a white plastic arena (40x20x20cm), divided into three chambers by separators with small circular openings and lined with fresh bedding, for 10 minutes. The left and right chamber contained empty wire-mesh cages. These were then used to display an age- and sex-matched conventionally-raised mouse (chamber 1) or a mouse-sized and –coloured (white) non-social object during the test phase (porcelain egg cup). Exploration of the 3 chambers by the test mouse was recorded on video

for 10 minutes and time spent in active interaction with the conspecific or object was measured by an experimenter, blinded to colonization status of the test mice. Group size for behaviour was n=12 for GF-SI mice and n=11 per group for CON-SI and exGF-SI groups, after removing outliers.

RNA extraction and sequencing

The amygdala from the left brain hemisphere was rapidly dissected on ice from fresh brain tissue as adapted from [80], stored in RNA*later* RNA Stabilization Reagent (Qiagen) at 4°C for 24 hours and then transferred to -80°C. Total RNA was extracted using the *mir*Vana™ miRNA Isolation kit (Ambion/life technologies) and DNase treated (Turbo DNA-free, Ambion/life technologies) according to the manufacturers recommendations For each group (CON, GF, exGF, CON-SI, GF-SI, exGF-SI), 8-12 animals were used (see Table 1 for details). RNA concentration and quality were determined using a Nanodrop 1000 (Thermo Scientific) and a Bioanalyzer (Agilent) was used to measure RNA integrity. After this, for all naïve groups equal amounts of RNA from two animals were then pooled to yield four samples per group. Therefore, for naïve groups, each sample (technical replicate) analysed by RNA-seq represents the average of two biological replicates.

Ribodepletion and library preparation was performed by Vertis Biotechnology (Freising, Germany). Sequencing as well as Fastq-file generation was done by Beckman Coulter Genomics service (Danvers, MA, USA). Stranded, paired-end reads of 2x100bp were produced on an Illumina HiSeq2500 sequencer. Details on RNA sample quality and sequencing quality control are given in **Supplementary File 8**.

Molecular validation by quantitative real-time PCR (qRT-PCR) for selected differentially regulated genes

To validate differential expression results by the RNAseq pipeline, we performed qRT-PCR analysis of all individual RNA samples for the six groups for 18 selected genes (**Fig. S2**). 61 % of comparisons showed matching results between the two methods. qRT-PCR was

400 performed as previously described [45]. In brief, qRT-PCR of 3 technical replicates was done
401 for each biological sample on a LightCycler 480 system (Roche LifeScience) and analysed
402 using the $\Delta\Delta C_t$ – method. Two-way ANOVA with multiple-testing correction (Tukey *post-hoc*
403 for effect of colonisation status; Sidak *post-hoc* for effect of social interaction stimulation),
404 was used to test for statistical significance between groups for each gene. Significance level
405 was: $p_{adj}<0.05$.
406
407 **Bioinformatic analysis pipeline**
408 *Quality control and mapping to reference genome*
409 Fastq-format reads were quality filtered and trimmed using Trimmomatic (v0.32,
410 RRID:SCR_011848) [81] with the following non-default parameters: *AVGQUAL*: 20;
411 *SLIDINGWINDOW*: 4:20; *LEADING*: 10; *TRAILING*: 10; *MINLEN*: 60. Alignment to the
412 mouse reference genome (GRCm38.p3) was achieved using the STAR aligner (v2.4.0f1)
413 [82] with default options and an index compiled with gene models retrieved from the Ensembl
414 database (release 78).
415
416 *Differential gene expression and functional enrichment analyses*
417 Ensembl database release 78 gene models were also used for counting mapped reads per
418 gene using HTSeq-Count (v0.6.0, RRID:SCR_011867) [83] with the following non-default
419 parameters: -s: no; -r: pos; -q –f bam –m intersection-nonempty. Differential gene expression
420 was calculated for pairwise comparisons using the DESeq2 R-package (v1.6.2) [84,85] with
421 default parameters. Genes with an FDR-adjusted p-value ≤ 0.1 were considered differentially
422 regulated. The data discussed in this publication have been deposited in NCBI's Gene
423 Expression Omnibus [86] and are accessible through GEO Series accession number
424 GSE114702 (https://www.ncbi.nlm.nih.gov/geo/query/acc.cgi?acc=GSE114702).
425

Differentially expressed genes were further analysed for functional enrichment using the DAVID Bioinformatic Resources (v6.7) [87,88] and Gene Set Enrichment Analysis (GSEA) (v2.0.14, RRID:SCR_003199) [89].

Differential exon usage analysis

For detection of differential exon usage the DEXSeq R-package was used (v1.12.2, RRID:SCR_012823) [90] with default parameters. FDR-corrected p-value significance level was set to 0.1. Ensemble database release 78 was used to provide exon models.

Statistics

Graphpad Prism (v6.0h, RRID:SCR_002798) was used for statistical hypothesis testing of behavioural analysis (**Fig. 1**) and expression of RNA processing genes (**Fig. 3D**). Before hypothesis testing on behavioural data, normal distribution was confirmed by D'Agostino & Pearson omnibus normality, Shapiro-Wilk normality, and KS normality tests ($p<0.05$ for all three tests). Sample size of n=12 was based on a power calculation with an expected effect size of f=0.4, a significance level of $\alpha=0.05$ and a power of 0.8. A Grubbs test for outliers ($p<0.05$) identified one outlier each in CON-SI and exGF-SI groups. One-way ANOVA with Tukey's multiple comparisons post-hoc test was run to compare social interaction between the groups.

For hypothesis testing of expression of RNA processing genes non-parametric Friedman testing was performed with Dunn's multiple comparison post-hoc test to compare expression levels between groups.

Statistical significance for overlaps of differentially expressed genes in pairwise comparisons (**Fig. 2C,D**) was computed using a publicly available web service (http://nemates.org/MA/progs/overlap_stats.html), which is based on the hypergeometric distribution and Fischer's exact test.

Heatmaps for functional enrichment (**Fig. 2E, Fig. 4D**): FDR-adjusted p-values were calculated for all enriched ($p_{adj}<0.1$) biological-function GO Terms using DAVID Bioinformatic

Resources (v6.7) (see above) and log-transformed ($-\log_{10}$) and colour-coded using Microsoft Excel (v15).

Pearson correlation coefficient for correlation between behavioural performance and gene expression level in individual mice was calculated using Microsoft Excel (v15).

Acknowledgements

The authors wish to thank Mr. Patrick Fitzgerald, and Ms. Frances O'Brien for technical assistance with animal husbandry, tissue extraction, and RNA extraction. The APC Microbiome Institute is a research centre funded by Science Foundation Ireland (SFI), through the Irish Government's National Development Plan (Grant Number 12/RC/2273). R.M.S. was supported by the Irish Research Council (IRC) through a Government of Ireland Postdoctoral Fellowship (Grant Number GOIPD/2014/355). M.J.C and F.J.R. are also supported by Science Foundation Ireland (Grant Number 11/SIRG/B2162.) T. G. D. and J. F. C. are also supported by the Irish Health Research Board, the Dept. of Agriculture, Food & Fisheries and Forestry and Enterprise Ireland. GC is supported by a NARSAD Young Investigator Grant from the Brain and Behavior Research Foundation (Grant Number 20771).

Conflict of interest statement

R.M.S, F.J.R., and A.E.H. report no biomedical financial interests or potential conflicts of interest. F.S., T.G.D., and J.F.C. are principal investigators in the APC Microbiome Institute, University College Cork. G.C. and M.C. are faculty member or funded investigator, respectively, of the APC Microbiome Institute. The APC Microbiome Institute has conducted research funded by Pfizer, GlaxoSmithKline, Proctor & Gamble, Mead Johnson, Suntory Wellness, and Cremo. T.G.D. has been an invited speaker at meetings organized by Servier, Lundbeck, Janssen, and AstraZeneca. J.F.C. has been an invited speaker at meetings organized by Mead Johnson, Yakult, Alkermes, and Janssen.

Figures

Figure 1: Germ-free (GF) mice display reduced social interaction. (A) Experimental design. **(B)** Time spent in active interaction with either a conspecific or non-social object in the 3-chamber social interaction test (3CSIT). Error bars show range, midlines of boxes show medians. (C) Results of the 2-way ANOVA with Dunnets multiple comparison *post-hoc* test, n=11-12/group).

Figure 2: Social interaction induces diverging gene expression patterns in the amygdala. (A) Number of differentially expressed genes (DEGs) including both up- and downregulated genes for all meaningful pairwise comparisons (see Table 1). **(B)** Presence-absence plot for all DEGs in all groups. Each line represents one gene that is a DEG in at least one pairwise comparison. **(C-D)** Venn diagram of upregulated (up, red) and downregulated (down, blue) genes in CON-GF and CON-SI or GF-SI comparisons to test for activation of expression patterns in GF mice under naïve conditions that are similar to activation by social interaction at either CON or GF colonisation status. **(E)** Heatmap to visualize enriched biological functions in social interaction(SI)-induced (upregulated only) genes. FDR-adjusted p-values were calculated for all enriched ($p_{adj}<0.1$) biological-function GO Terms (GObp), log-transformed ($-\log_{10}$) and colour-coded.

Figure 3: Loss of normal induction of MAP-K pathway is accompanied by upregulation of splicing pathways. (A) Comparison of enrichment of MAP-K pathway-associated genes and spliceosome-related genes among DEGs between groups. Dotted line: significance level (p=0.1) **(B)** Functional enrichment analysis of overlapping and uniquely regulated subsets of DEGs between CON-SI and GF-SI comparisons showed shared and different processes transcriptionally activated in the amygdala in response to social stimulation **(C)** Percentage of DEGs falling into the TOP20 enriched KEGG pathways for CON-SI and GF-SI. **(D)** Log_2(fold change) (Log2FC) values plotted for each of the 112 DEGs in the GF-SI comparison that was associated with GO-Term “RNA processing”. black line: median, non-parametric

Friedman test F=65.5, p<1.0e-4; ***p<1.0e-4, *p<0.05, Dunn's multiple comparisons, n=112/group.

Figure 4: Social interaction leads to a strong increase in alternative splicing in GF and exGF animals. (A) Number of differentially spliced genes (DSGs) for all meaningful pairwise comparisons (see Table 1). **(B-C)** Venn diagrams showing overlapping DSGs for naïve (B) and social interaction (SI, C) comparisons. After stimulation differences become evident. **(D)** Heatmap to visualize enriched pathways in SI-induced differentially spliced genes. FDR-adjusted p-values were calculated for all enriched (p_{adj}<0.1) KEGG pathways, log-transformed ($-\log_{10}$) and colour-coded.

Figure 5: Behavioural performance correlates with expression of RNA processing genes in GF mice. (A) Design of analysis. A gene list, ranked by Pearson correlation between expression level of a given gene and behavioural performance for each individual mouse, was used for gene-set enrichment analysis (GSEA). The algorithm assigns one or multiple functions to each gene in the list based on the GO-Term or KEGG Pathway databases, then calculates an enrichment score for each function based on the rank of genes associated with this function **(B-C)** GSEA-generated enrichment plots for two selected significantly enriched functions (KEGG pathway "Spliceosome", GO-Term "RNA splicing"). **(D)** Normalized GSEA enrichment scores for all significantly enriched functions or pathways found in this analysis. (**E**) Gene-expression analysis within the GF-SI group (GF-SI^{high} vs GF-SI^{low}, n=6). Shown are expression values for 3 significantly differentially regulated genes plotted against the animals time spent in active social interaction. r: Pearson correlation coefficient

Tables *(embedded in document)*

Table 1: Meaningful pairwise comparisons for gene expression changes (9 unique comparisons)

Supplementary material

- **Figure 2-figure supplement 1 (A)** Results of differential gene expression analysis using more stringent filter criteria (padj<0.1 and log2(fold-change)>0.5 or <-0.5) as compared to Fig. 1, where filter criteria are padj<0.1. Left panel: Number of differentially expressed genes (DEGs, both directions), right panel: Enrichment of KEGG pathways “MAPK sig. pathway” and “Spliceosome” (expressed as –log10(padj)). **(B)** Log2(fold-change)-values for all genes associated with the GO-Term “RNA processing” for all comparisons after social interaction (SI). Each line represents one gene, genes significantly up-/downregulated in GF-SI comparison are highlighted in yellow, which are the same genes shown in Fig. 3D. **(C)** Comparison of genes induced by SI in the murine amygdala with genes induced by environmental novelty in the murine hippocampus (see ref. Stilling et al. 2014, EMBO J). Overlapping upregulated genes are listed and genes with similar function are grouped using different colours.
- **Figure 2-figure supplement 2 (A)** RT-qPCR validation results for 18 selected genes. n=4-12 per group**. (B)** Overview of correspondence of RNAseq and qPCR results for selected genes. RT-qPCR results were analysed by 2-way ANOVA with multiple-testing correction (Tukey correction for effect of colonisation status; Sidak correction for effect of social interaction stimulation (SI)), significance level: padj<0.05
- **Supplementary File 1: Differentially expressed genes**
- **Supplementary File 2: Functional enrichment DEGs**
- **Supplementary File 3: DEGs GO-heatmap**
- **Supplementary File 4: DSGs**
- **Supplementary File 5: Functional enrichment DSGs**
- **Supplementary File 6: DSGs KEGG-heatmap**
- **Supplementary File 7: Correlation gene expression with behaviour**
- **Supplementary File 8: Details on RNA sample quality and sequencing quality control**

- **Supplementary File 9: Raw FastQC quality control files for sequencing data**

References

1. Collins SM, Surette M, Bercik P. The interplay between the intestinal microbiota and the brain. Nat Rev Microbiol. 2012;10:735–42.
2. Cryan JF, Dinan TG. Mind-altering microorganisms: the impact of the gut microbiota on brain and behaviour. Nat Rev Neurosci. 2012;13:701–12.
3. Foster JA, Rinaman L, Cryan JF. Stress & the gut-brain axis: Regulation by the microbiome. Neurobiol Stress [Internet]. 2017; Available from: http://www.sciencedirect.com/science/article/pii/S2352289516300509
4. Lyte M. Microbial Endocrinology in the Microbiome-Gut-Brain Axis: How Bacterial Production and Utilization of Neurochemicals Influence Behavior. PLoS Pathog. 2013;9:e1003726.
5. Mayer EA, Knight R, Mazmanian SK, Cryan JF, Tillisch K. Gut microbes and the brain: paradigm shift in neuroscience. J Neurosci Off J Soc Neurosci. 2014;34:15490–6.
6. Sampson TR, Mazmanian SK. Control of brain development, function, and behavior by the microbiome. Cell Host Microbe. 2015;17:565–76.
7. Sharon G, Sampson TR, Geschwind DH, Mazmanian SK. The Central Nervous System and the Gut Microbiome. Cell. 2016;167:915–32.
8. Arentsen T, Raith H, Qian Y, Forssberg H, Diaz-Heijtz R. Host microbiota modulates development of social preference in mice. Microb Ecol Health Dis [Internet]. 2015 [cited 2015 Dec 21];26. Available from: http://www.microbecolhealthdis.net/index.php/mehd/article/view/29719
9. Crumeyrolle-Arias M, Jaglin M, Bruneau A, Vancassel S, Cardona A, Daugé V, et al. Absence of the gut microbiota enhances anxiety-like behavior and neuroendocrine response to acute stress in rats. Psychoneuroendocrinology. 2014;42:207–17.
10. de Theije CGM, Wopereis H, Ramadan M, van Eijndthoven T, Lambert J, Knol J, et al. Altered gut microbiota and activity in a murine model of autism spectrum disorders. Brain Behav Immun. 2014;37:197–206.
11. Desbonnet L, Clarke G, Shanahan F, Dinan TG, Cryan JF. Microbiota is essential for social development in the mouse. Mol Psychiatry. 2014;19:146–8.
12. Ezenwa VO, Gerardo NM, Inouye DW, Medina M, Xavier JB. Animal Behavior and the Microbiome. Science. 2012;338:198–9.
13. Gacias M, Gaspari S, Santos P-MG, Tamburini S, Andrade M, Zhang F, et al. Microbiota-driven transcriptional changes in prefrontal cortex override genetic differences in social behavior. eLife. 2016;5:e13442.
14. Kwong WK, Medina LA, Koch H, Sing K-W, Soh EJY, Ascher JS, et al. Dynamic microbiome evolution in social bees. Sci Adv. 2017;3:e1600513.
15. Leclaire S, Jacob S, Greene LK, Dubay GR, Drea CM. Social odours covary with bacterial community in the anal secretions of wild meerkats. Sci Rep. 2017;7:3240.
16. Lewin-Epstein O, Aharonov R, Hadany L. Microbes can help explain the evolution of host altruism. Nat Commun. 2017;8:14040.
17. Montiel-Castro AJ, González-Cervantes RM, Bravo-Ruiseco G, Pacheco-López G. The microbiota–gut–brain axis: neurobehavioral correlates, health and sociality. Front Integr Neurosci. 2013;7:70.
18. Montiel-Castro null, Augusto J, Baez-Yanez null, Mario G, Pacheco-Lopez G. Social neuroeconomics: the influence of microbiota in partner-choice and sociality. Curr Pharm Des. 2014;20:4774–83.
19. Parashar A, Udayabanu M. Gut microbiota regulates key modulators of social behavior. Eur Neuropsychopharmacol. 2016;26:78–91.
20. Sharon G, Segal D, Ringo JM, Hefetz A, Zilber-Rosenberg I, Rosenberg E. Commensal bacteria play a role in mating preference of Drosophila melanogaster. Proc Natl Acad Sci. 2010;107:20051–6.
21. Snyder-Mackler N, Sanz J, Kohn JN, Brinkworth JF, Morrow S, Shaver AO, et al. Social status alters immune regulation and response to infection in macaques. Science. 2016;354:1041–5.

614 22. Stilling RM, Bordenstein SR, Dinan TG, Cryan JF. Friends with social benefits: host-microbe
615 interactions as a driver of brain evolution and development? Front Cell Infect Microbiol. 2014;4:147.
616 23. Theis KR, Venkataraman A, Dycus JA, Koonter KD, Schmitt-Matzen EN, Wagner AP, et al.
617 Symbiotic bacteria appear to mediate hyena social odors. Proc Natl Acad Sci. 2013;110:19832–7.
618 24. Tung J, Barreiro LB, Burns MB, Grenier J-C, Lynch J, Grieneisen LE, et al. Social networks
619 predict gut microbiome composition in wild baboons. eLife. 2015;4:e05224.
620 25. Tillisch K, Labus J, Kilpatrick L, Jiang Z, Stains J, Ebrat B, et al. Consumption of Fermented Milk
621 Product With Probiotic Modulates Brain Activity. Gastroenterology. 2013;144:1394-1401.e4.
622 26. Hsiao EY, McBride SW, Hsien S, Sharon G, Hyde ER, McCue T, et al. Microbiota modulate
623 behavioral and physiological abnormalities associated with neurodevelopmental disorders. Cell.
624 2013;155:1451–63.
625 27. Kang D-W, Adams JB, Gregory AC, Borody T, Chittick L, Fasano A, et al. Microbiota Transfer
626 Therapy alters gut ecosystem and improves gastrointestinal and autism symptoms: an open-label
627 study. Microbiome. 2017;5:10.
628 28. Mayer EA, Padua D, Tillisch K. Altered brain-gut axis in autism: comorbidity or causative
629 mechanisms? BioEssays News Rev Mol Cell Dev Biol. 2014;36:933–9.
630 29. Strati F, Cavalieri D, Albanese D, De Felice C, Donati C, Hayek J, et al. New evidences on the
631 altered gut microbiota in autism spectrum disorders. Microbiome. 2017;5:24.
632 30. Dinan TG, Borre YE, Cryan JF. Genomics of schizophrenia: time to consider the gut microbiome?
633 Mol Psychiatry. 2014;19:1252–7.
634 31. Golubeva AV, Joyce SA, Moloney G, Burokas A, Sherwin E, Arboleya S, et al. Microbiota-related
635 Changes in Bile Acid & Tryptophan Metabolism are Associated With Gastrointestinal Dysfunction in
636 a Mouse Model of Autism. EBioMedicine [Internet]. 2017 [cited 2017 Sep 27];0. Available from:
637 http://www.ebiomedicine.com/article/S2352-3964(17)30374-2/fulltext
638 32. Kim S, Kim H, Yim YS, Ha S, Atarashi K, Tan TG, et al. Maternal gut bacteria promote
639 neurodevelopmental abnormalities in mouse offspring. Nature. 2017;549:528–32.
640 33. Allsop SA, Vander Weele CM, Wichmann R, Tye KM. Optogenetic insights on the relationship
641 between anxiety-related behaviors and social deficits. Front Behav Neurosci. 2014;8:241.
642 34. Amaral DG. The amygdala, social behavior, and danger detection. Ann N Y Acad Sci.
643 2003;1000:337–47.
644 35. Kliemann D, Dziobek I, Hatri A, Baudewig J, Heekeren HR. The role of the amygdala in atypical
645 gaze on emotional faces in autism spectrum disorders. J Neurosci Off J Soc Neurosci. 2012;32:9469–
646 76.
647 36. Noonan MP, Sallet J, Mars RB, Neubert FX, O'Reilly JX, Andersson JL, et al. A neural circuit
648 covarying with social hierarchy in macaques. PLoS Biol. 2014;12:e1001940.
649 37. Phelps EA, LeDoux JE. Contributions of the Amygdala to Emotion Processing: From Animal
650 Models to Human Behavior. Neuron. 2005;48:175–87.
651 38. Sabatini MJ, Ebert P, Lewis DA, Levitt P, Cameron JL, Mirnics K. Amygdala gene expression
652 correlates of social behavior in monkeys experiencing maternal separation. J Neurosci Off J Soc
653 Neurosci. 2007;27:3295–304.
654 39. Sallet J, Mars RB, Noonan MP, Andersson JL, O'Reilly JX, Jbabdi S, et al. Social Network Size
655 Affects Neural Circuits in Macaques. Science. 2011;334:697–700.
656 40. Amaral DG, Corbett BA. The amygdala, autism and anxiety. Novartis Found Symp.
657 2003;251:177–87; discussion 187-197, 281–97.
658 41. Baron-Cohen S, Ring HA, Bullmore ET, Wheelwright S, Ashwin C, Williams SC. The amygdala
659 theory of autism. Neurosci Biobehav Rev. 2000;24:355–64.
660 42. Monk CS, Weng S-J, Wiggins JL, Kurapati N, Louro HMC, Carrasco M, et al. Neural circuitry of
661 emotional face processing in autism spectrum disorders. J Psychiatry Neurosci JPN. 2010;35:105–14.
662 43. Schultz RT. Developmental deficits in social perception in autism: the role of the amygdala and
663 fusiform face area. Int J Dev Neurosci Off J Int Soc Dev Neurosci. 2005;23:125–41.
664 44. Hoban AE, Stilling RM, Moloney G, Shanahan F, Dinan TG, Clarke G, et al. The microbiome
665 regulates amygdala-dependent fear recall. Mol Psychiatry [Internet]. 2017 [cited 2017 May 19];
666 Available from: https://www.nature.com/mp/journal/vaop/ncurrent/full/mp2017100a.html
667 45. Stilling RM, Ryan FJ, Hoban AE, Shanahan F, Clarke G, Claesson MJ, et al. Microbes &
668 neurodevelopment - Absence of microbiota during early life increases activity-related transcriptional
669 pathways in the amygdala. Brain Behav Immun. 2015;50:209–20.

46. Luczynski P, Whelan SO, O'Sullivan C, Clarke G, Shanahan F, Dinan TG, et al. Adult microbiota-deficient mice have distinct dendritic morphological changes: differential effects in the amygdala and hippocampus. Eur J Neurosci. 2016;44:2654–66.
47. Hoban AE, Stilling RM, M. Moloney G, Moloney RD, Shanahan F, Dinan TG, et al. Microbial regulation of microRNA expression in the amygdala and prefrontal cortex. Microbiome [Internet]. 2017 [cited 2017 Aug 22];5. Available from: http://microbiomejournal.biomedcentral.com/articles/10.1186/s40168-017-0321-3
48. Bäckhed F, Manchester JK, Semenkovich CF, Gordon JI. Mechanisms underlying the resistance to diet-induced obesity in germ-free mice. Proc Natl Acad Sci. 2007;104:979–84.
49. Bercik P, Denou E, Collins J, Jackson W, Lu J, Jury J, et al. The intestinal microbiota affect central levels of brain-derived neurotropic factor and behavior in mice. Gastroenterology. 2011;141:599–609, 609.e1-3.
50. Clarke G, Grenham S, Scully P, Fitzgerald P, Moloney RD, Shanahan F, et al. The microbiome-gut-brain axis during early life regulates the hippocampal serotonergic system in a sex-dependent manner. Mol Psychiatry. 2013;18:666–73.
51. Diaz Heijtz R, Wang S, Anuar F, Qian Y, Björkholm B, Samuelsson A, et al. Normal gut microbiota modulates brain development and behavior. Proc Natl Acad Sci U S A. 2011;108:3047–52.
52. McVey Neufeld KA, Mao YK, Bienenstock J, Foster JA, Kunze WA. The microbiome is essential for normal gut intrinsic primary afferent neuron excitability in the mouse. Neurogastroenterol Motil Off J Eur Gastrointest Motil Soc. 2013;25:183-e88.
53. Neufeld KM, Kang N, Bienenstock J, Foster JA. Reduced anxiety-like behavior and central neurochemical change in germ-free mice. Neurogastroenterol Motil. 2011;23:255-e119.
54. Ridaura VK, Faith JJ, Rey FE, Cheng J, Duncan AE, Kau AL, et al. Gut Microbiota from Twins Discordant for Obesity Modulate Metabolism in Mice. Science. 2013;341:1241214.
55. Luczynski P, McVey Neufeld K-A, Oriach CS, Clarke G, Dinan TG, Cryan JF. Growing up in a Bubble: Using Germ-Free Animals to Assess the Influence of the Gut Microbiota on Brain and Behavior. Int J Neuropsychopharmacol. 2016;19.
56. Stilling RM, Dinan TG, Cryan JF. Microbial genes, brain & behaviour - epigenetic regulation of the gut-brain axis. Genes Brain Behav. 2014;13:69–86.
57. Gareau MG, Wine E, Rodrigues DM, Cho JH, Whary MT, Philpott DJ, et al. Bacterial infection causes stress-induced memory dysfunction in mice. Gut. 2011;60:307–17.
58. Nadler JJ, Moy SS, Dold G, Trang D, Simmons N, Perez A, et al. Automated apparatus for quantitation of social approach behaviors in mice. Genes Brain Behav. 2004;3:303–14.
59. Buffington SA, Di Prisco GV, Auchtung TA, Ajami NJ, Petrosino JF, Costa-Mattioli M. Microbial Reconstitution Reverses Maternal Diet-Induced Social and Synaptic Deficits in Offspring. Cell. 2016;165:1762–75.
60. Subramanian A, Tamayo P, Mootha VK, Mukherjee S, Ebert BL, Gillette MA, et al. Gene set enrichment analysis: a knowledge-based approach for interpreting genome-wide expression profiles. Proc Natl Acad Sci U S A. 2005;102:15545–50.
61. Sliwa J, Freiwald WA. A dedicated network for social interaction processing in the primate brain. Science. 2017;356:745–9.
62. Arseneault-Bréard J, Rondeau I, Gilbert K, Girard S-A, Tompkins TA, Godbout R, et al. Combination of Lactobacillus helveticus R0052 and Bifidobacterium longum R0175 reduces post-myocardial infarction depression symptoms and restores intestinal permeability in a rat model. Br J Nutr. 2012;107:1793–9.
63. Bercik P, Verdu EF, Foster JA, Macri J, Potter M, Huang X, et al. Chronic gastrointestinal inflammation induces anxiety-like behavior and alters central nervous system biochemistry in mice. Gastroenterology. 2010;139:2102-2112.e1.
64. Gilbert K, Arseneault-Bréard J, Flores Monaco F, Beaudoin A, Bah TM, Tompkins TA, et al. Attenuation of post-myocardial infarction depression in rats by n-3 fatty acids or probiotics starting after the onset of reperfusion. Br J Nutr. 2013;109:50–6.
65. Arentsen T, Qian Y, Gkotzis S, Femenia T, Wang T, Udekwu K, et al. The bacterial peptidoglycan-sensing molecule Pglyrp2 modulates brain development and behavior. Mol Psychiatry. 2017;22:257–66.
66. Koch H, Schmid-Hempel P. Socially transmitted gut microbiota protect bumble bees against an intestinal parasite. Proc Natl Acad Sci U S A. 2011;108:19288–92.

67. Wang Q, Sawyer IA, Sung M-H, Sturgill D, Shevtsov SP, Pegoraro G, et al. Cajal bodies are linked to genome conformation. Nat Commun. 2016;7:10966.
68. Lafarga M, Tapia O, Romero AM, Berciano MT. Cajal bodies in neurons. RNA Biol. 2016;1–14.
69. Stilling RM, Rönicke R, Benito E, Urbanke H, Capece V, Burkhardt S, et al. K-Lysine acetyltransferase 2a regulates a hippocampal gene expression network linked to memory formation. EMBO J. 2014;33:1912–27.
70. Schafer DP, Lehrman EK, Kautzman AG, Koyama R, Mardinly AR, Yamasaki R, et al. Microglia Sculpt Postnatal Neural Circuits in an Activity and Complement-Dependent Manner. Neuron. 2012;74:691–705.
71. Stephan AH, Barres BA, Stevens B. The complement system: an unexpected role in synaptic pruning during development and disease. Annu Rev Neurosci. 2012;35:369–89.
72. Stevens B, Allen NJ, Vazquez LE, Howell GR, Christopherson KS, Nouri N, et al. The classical complement cascade mediates CNS synapse elimination. Cell. 2007;131:1164–78.
73. Gupta S, Ellis SE, Ashar FN, Moes A, Bader JS, Zhan J, et al. Transcriptome analysis reveals dysregulation of innate immune response genes and neuronal activity-dependent genes in autism. Nat Commun. 2014;5:5748.
74. Ding X, Liu S, Tian M, Zhang W, Zhu T, Li D, et al. Activity-induced histone modifications govern Neurexin-1 mRNA splicing and memory preservation. Nat Neurosci. 2017;20:690–9.
75. Hermey G, Blüthgen N, Kuhl D. Neuronal activity-regulated alternative mRNA splicing. Int J Biochem Cell Biol. 2017;
76. Iijima T, Hidaka C, Iijima Y. Spatio-temporal regulations and functions of neuronal alternative RNA splicing in developing and adult brains. Neurosci Res. 2016;109:1–8.
77. Schor IE, Rascovan N, Pelisch F, Alló M, Kornblihtt AR. Neuronal cell depolarization induces intragenic chromatin modifications affecting NCAM alternative splicing. Proc Natl Acad Sci. 2009;106:4325–30.
78. Quesnel-Vallières M, Dargaei Z, Irimia M, Gonatopoulos-Pournatzis T, Ip JY, Wu M, et al. Misregulation of an Activity-Dependent Splicing Network as a Common Mechanism Underlying Autism Spectrum Disorders. Mol Cell. 2016;64:1023–34.
79. O'Tuathaigh CMP, Babovic D, O'Sullivan GJ, Clifford JJ, Tighe O, Croke DT, et al. Phenotypic characterization of spatial cognition and social behavior in mice with "knockout" of the schizophrenia risk gene neuregulin 1. Neuroscience. 2007;147:18–27.
80. Zapala MA, Hovatta I, Ellison JA, Wodicka L, Rio JAD, Tennant R, et al. Adult mouse brain gene expression patterns bear an embryologic imprint. Proc Natl Acad Sci U S A. 2005;102:10357–62.
81. Bolger AM, Lohse M, Usadel B. Trimmomatic: a flexible trimmer for Illumina sequence data. Bioinforma Oxf Engl. 2014;30:2114–20.
82. Dobin A, Davis CA, Schlesinger F, Drenkow J, Zaleski C, Jha S, et al. STAR: ultrafast universal RNA-seq aligner. Bioinforma Oxf Engl. 2013;29:15–21.
83. Anders S, Pyl PT, Huber W. HTSeq--a Python framework to work with high-throughput sequencing data. Bioinforma Oxf Engl. 2015;31:166–9.
84. Anders S, Huber W. Differential expression analysis for sequence count data. Genome Biol. 2010;11:R106.
85. Love MI, Huber W, Anders S. Moderated estimation of fold change and dispersion for RNA-seq data with DESeq2. Genome Biol. 2014;15:550.
86. Edgar R, Domrachev M, Lash AE. Gene Expression Omnibus: NCBI gene expression and hybridization array data repository. Nucleic Acids Res. 2002;30:207–10.
87. Huang DW, Sherman BT, Lempicki RA. Bioinformatics enrichment tools: paths toward the comprehensive functional analysis of large gene lists. Nucleic Acids Res. 2009;37:1–13.
88. Huang DW, Sherman BT, Lempicki RA. Systematic and integrative analysis of large gene lists using DAVID bioinformatics resources. Nat Protoc. 2009;4:44–57.
89. Subramanian A, Kuehn H, Gould J, Tamayo P, Mesirov JP. GSEA-P: a desktop application for Gene Set Enrichment Analysis. Bioinforma Oxf Engl. 2007;23:3251–3.
90. Anders S, Reyes A, Huber W. Detecting differential usage of exons from RNA-seq data. Genome Res. 2012;22:2008–17.

Fig. 1

A

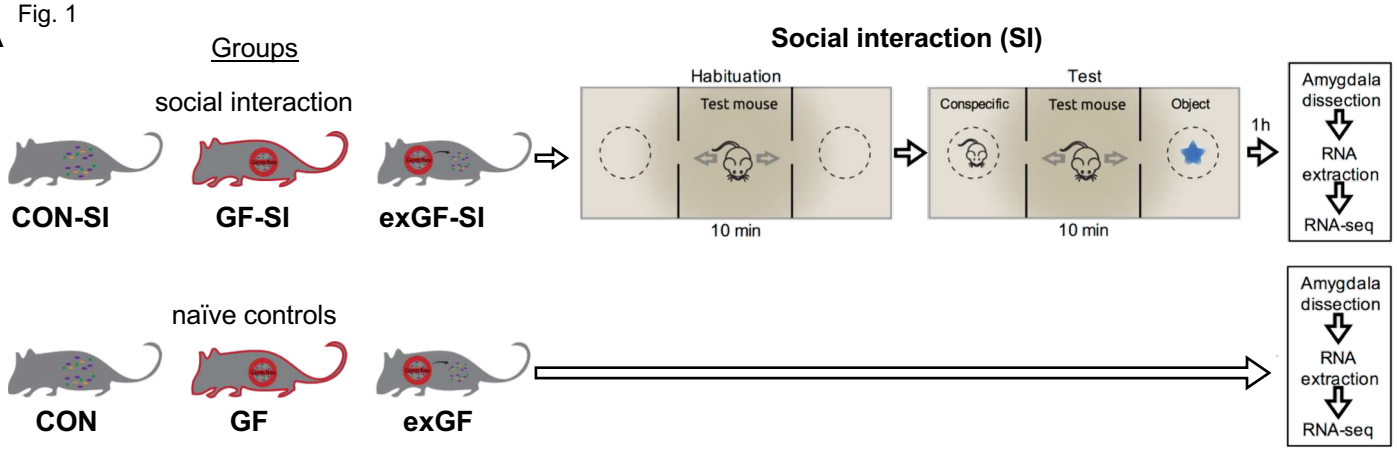

B

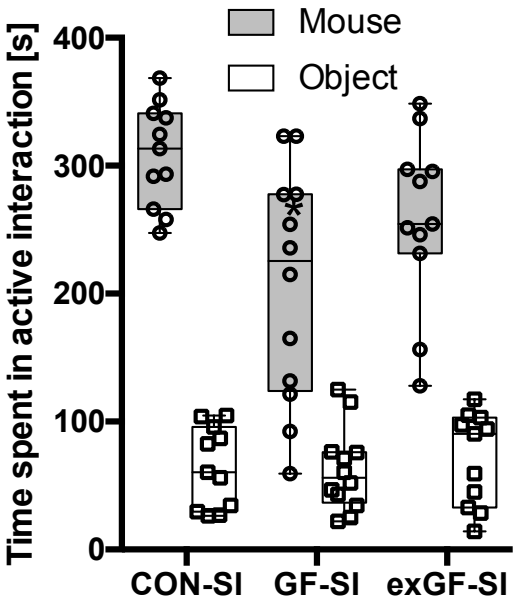

C

Effect of ...	F(DFn/DFd)	p-value
Time with Mouse/Object	F(1, 62) = 205.8	p<0.0001
Colonisation status (CON/GF/exGF)	F(2, 62) = 5.219	p=0.008
Interaction	F(2, 62) = 4.77	p=0.012
***post-hoc* tests**	**p-value (Dunnett's adjusted)**	
CON-SI vs GF-SI (Mouse)	p<0.0001	
CON-SI vs exGF-SI (Mouse)	p=0.06	

Fig. 2

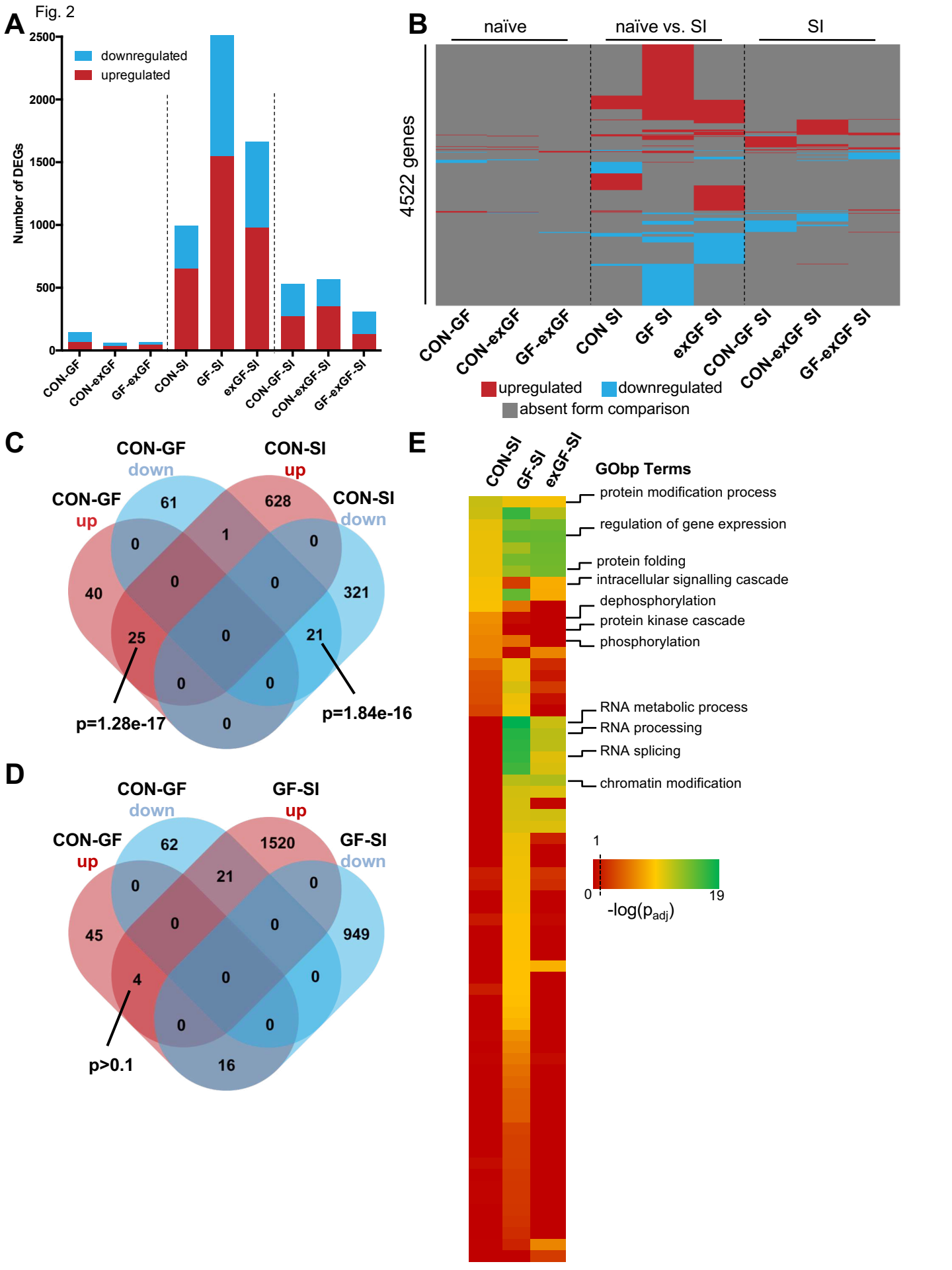
A
downregulated
upregulated
Number of DEGs
2500
2000
1500
1000
500
0
CON-GF
CON-exGF
GF-exGF
CON-SI
GF-SI
exGF-SI
CON-GF-SI
CON-exGF-SI
GF-exGF-SI
B
naïve
naïve vs. SI
SI
4522 genes
CON-GF
CON-exGF
GF-exGF
CON SI
GF SI
exGF SI
CON-GF SI
CON-exGF SI
GF-exGF SI
upregulated
downregulated
absent form comparison
C
CON-GF
down
CON-SI
up
CON-GF
up
CON-SI
down
61
628
1
0
0
0
0
40
321
25
0
21
0
0
0
p=1.28e-17
p=1.84e-16
D
CON-GF
down
GF-SI
up
CON-GF
up
GF-SI
down
62
1520
21
0
0
0
0
45
949
4
0
0
0
0
p>0.1
16
E
CON-SI
GF-SI
exGF-SI
GObp Terms
protein modification process
regulation of gene expression
protein folding
intracellular signalling cascade
dephosphorylation
protein kinase cascade
phosphorylation
RNA metabolic process
RNA processing
RNA splicing
chromatin modification
1
0
19
-log(padj)

A

More stringent filter criteria: p_{adj}<0.1, log_2(FC)>|±0.5|

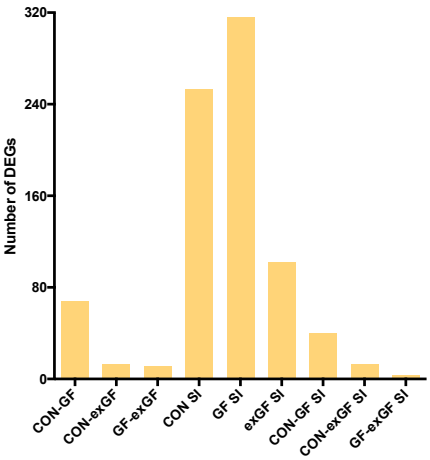

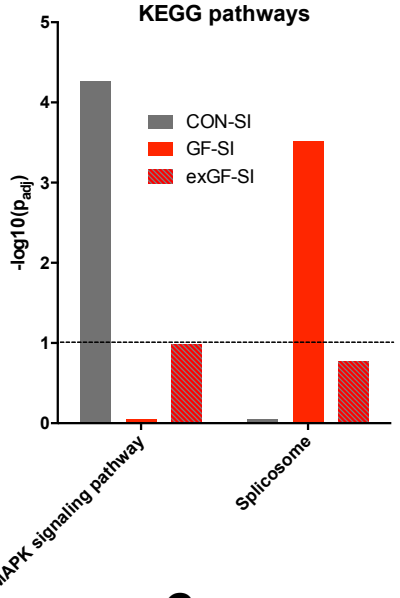

B

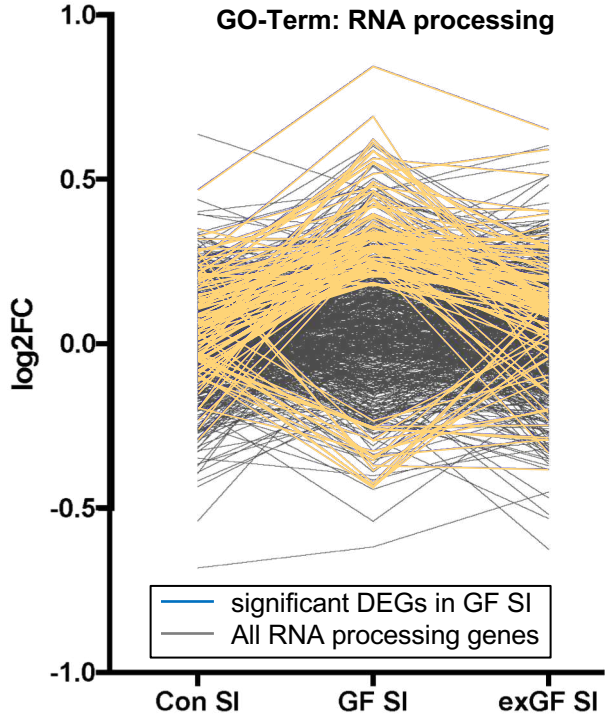

C

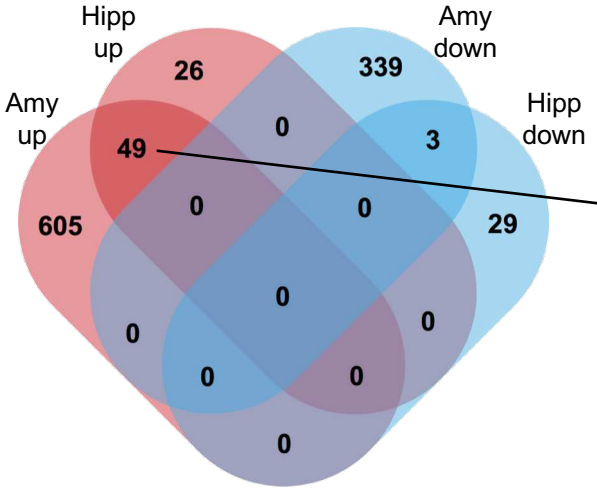

Adipor2
Arc
Arl4d
Arl5b
Cdkn1a
Coq10b
Dio2
Dnajb1
Dnajb5
Dusp4
Dusp6
Egr1
Egr2
Egr3
Egr4
Errfi1
Fam46a
Fos
Fosb
Fosl2
Gadd45b
Gpr3
Gpt2
Homer1
Ier5
Irs2
Kdm7a
Lingo3
Map3k19
Mfsd2a
Midn
Nfkbia
Nostrin
Nptx2
Nr4a3
Pcsk1
Per1
Per2
Plin4
Ppp1r3g
Prr5
Rrp8
Sertad1
Sik1
Slc2a1
Smim3
Tnfrsf12a
Tsc22d3
Zdbf2

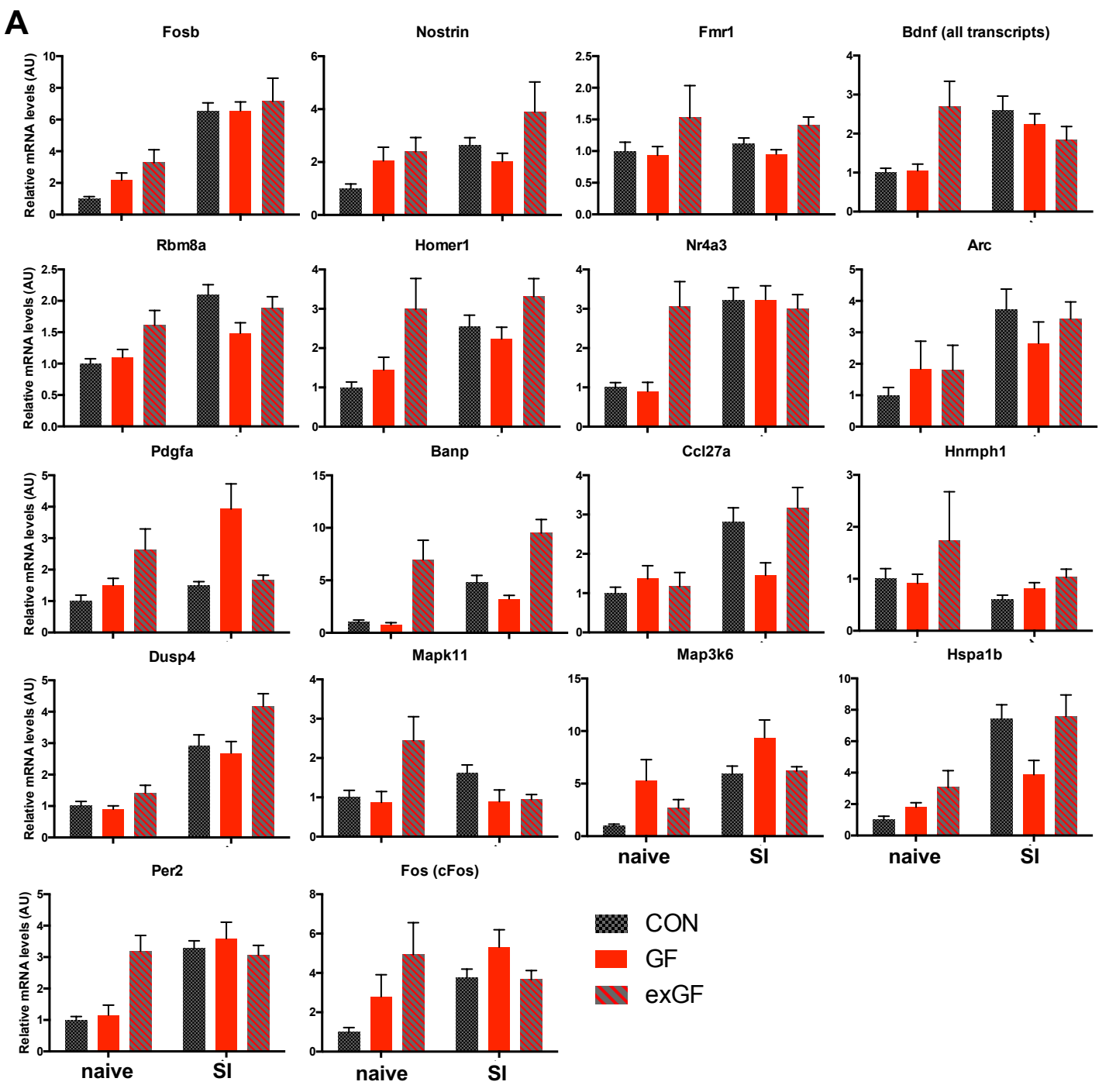

B

	Fosb	Nostrin	Fmr1	Map3k6	Homer1	Hspa1b	Pdgfa	Banp	Ccl27a	Dusp4	Rbm8a	Per2	Nr4a3	Fos	Mapk11	Bdnf_all	Hnrnph1	Arc
CON-GF																		
CON-exGF																		
GF-exGF																		
CON-CONsi																		
GF-GFsi																		
exGF-exGFsi																		

confirmed results	66	61%
opposite result	1	1%
results not confirmed	39	36%
Total	108	

Fig. 3

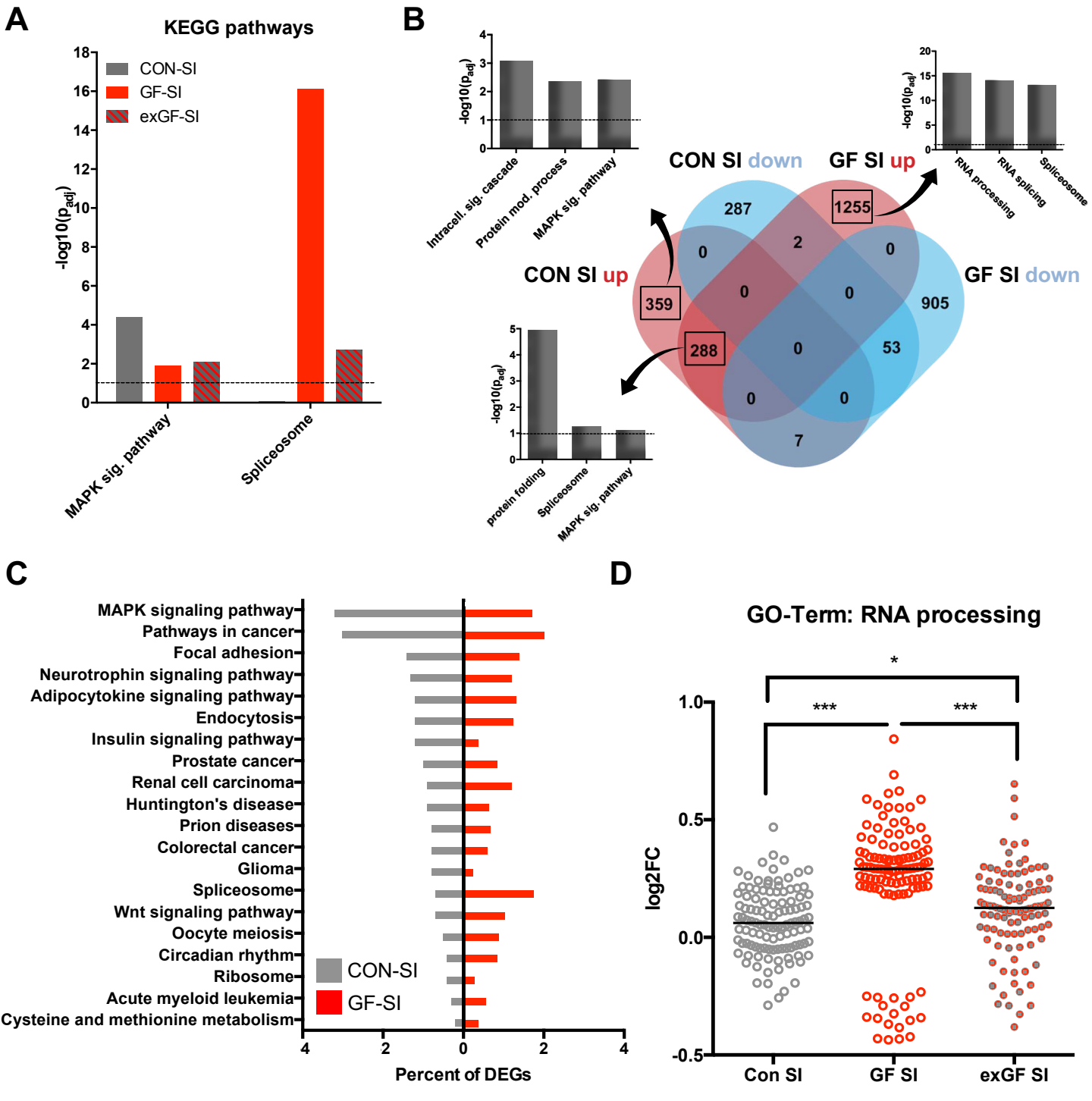
A
KEGG pathways
CON-SI
GF-SI
exGF-SI
-log10(padj)
MAPK sig. pathway
Spliceosome
B
-log10(padj)
Intracell. sig. cascade
Protein mod. process
MAPK sig. pathway
CON SI down
GF SI up
CON SI up
GF SI down
287
1255
2
0
0
0
0
359
905
288
53
0
0
7
-log10(padj)
RNA processing
RNA splicing
Spliceosome
-log10(padj)
protein folding
Spliceosome
MAPK sig. pathway
C
MAPK signaling pathway
Pathways in cancer
Focal adhesion
Neurotrophin signaling pathway
Adipocytokine signaling pathway
Endocytosis
Insulin signaling pathway
Prostate cancer
Renal cell carcinoma
Huntington's disease
Prion diseases
Colorectal cancer
Glioma
Spliceosome
Wnt signaling pathway
Oocyte meiosis
Circadian rhythm
Ribosome
Acute myeloid leukemia
Cysteine and methionine metabolism
CON-SI
GF-SI
Percent of DEGs
D
GO-Term: RNA processing
log2FC
Con SI
GF SI
exGF SI
*
***
***

Fig. 4

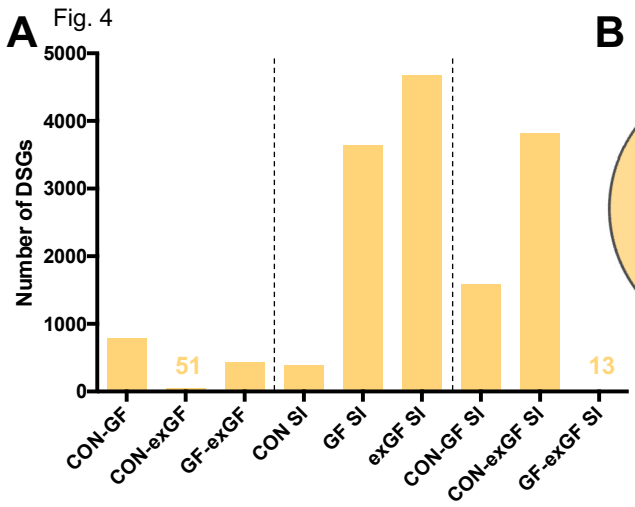
A
Number of DSGs
5000
4000
3000
2000
1000
0
51
13
CON-GF
CON-exGF
GF-exGF
CON SI
GF SI
exGF SI
CON-GF SI
CON-exGF SI
GF-exGF SI

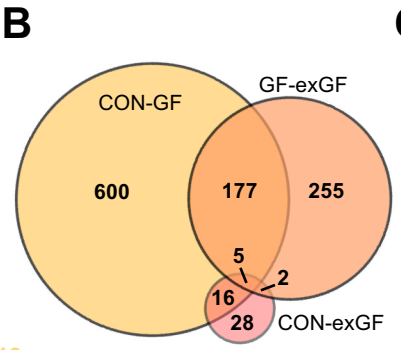
B
CON-GF
GF-exGF
600
177
255
5
2
16
28
CON-exGF

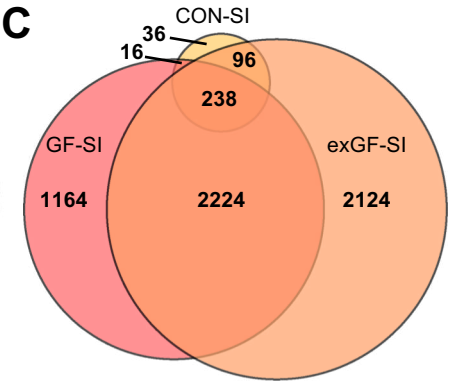
C
CON-SI
36
16
96
238
GF-SI
exGF-SI
1164
2224
2124

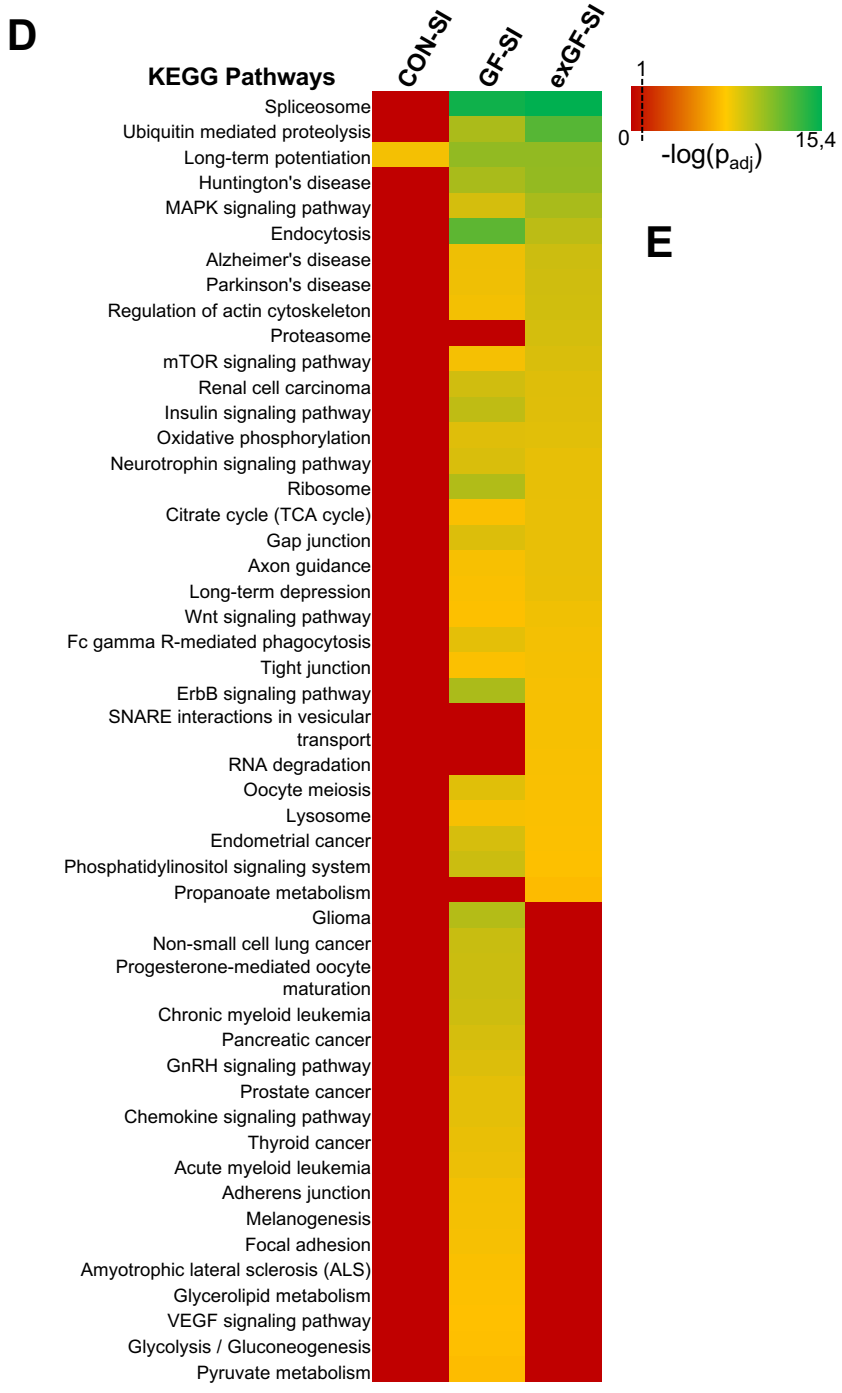
D
KEGG Pathways
CON-SI
GF-SI
exGF-SI
1
0
15,4
-log(padj)
E
Spliceosome
Ubiquitin mediated proteolysis
Long-term potentiation
Huntington's disease
MAPK signaling pathway
Endocytosis
Alzheimer's disease
Parkinson's disease
Regulation of actin cytoskeleton
Proteasome
mTOR signaling pathway
Renal cell carcinoma
Insulin signaling pathway
Oxidative phosphorylation
Neurotrophin signaling pathway
Ribosome
Citrate cycle (TCA cycle)
Gap junction
Axon guidance
Long-term depression
Wnt signaling pathway
Fc gamma R-mediated phagocytosis
Tight junction
ErbB signaling pathway
SNARE interactions in vesicular transport
RNA degradation
Oocyte meiosis
Lysosome
Endometrial cancer
Phosphatidylinositol signaling system
Propanoate metabolism
Glioma
Non-small cell lung cancer
Progesterone-mediated oocyte maturation
Chronic myeloid leukemia
Pancreatic cancer
GnRH signaling pathway
Prostate cancer
Chemokine signaling pathway
Thyroid cancer
Acute myeloid leukemia
Adherens junction
Melanogenesis
Focal adhesion
Amyotrophic lateral sclerosis (ALS)
Glycerolipid metabolism
VEGF signaling pathway
Glycolysis / Gluconeogenesis
Pyruvate metabolism

Fig. 5

A

Analysis design:

Gene list ranked by Pearson correlation (time spent with conspecific vs. gene expression) in the GF-SI group

(1) ---- → function
(2) ---- → function
(3) ---- → function
(4) ---- → function
(5) ---- → function
(6) ---- → function
(n) … ...

Gene set enrichment analysis (GSEA)

B

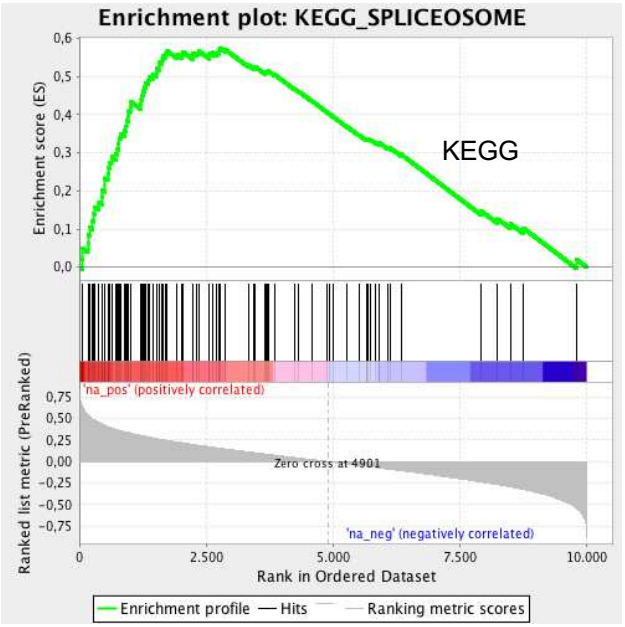

C

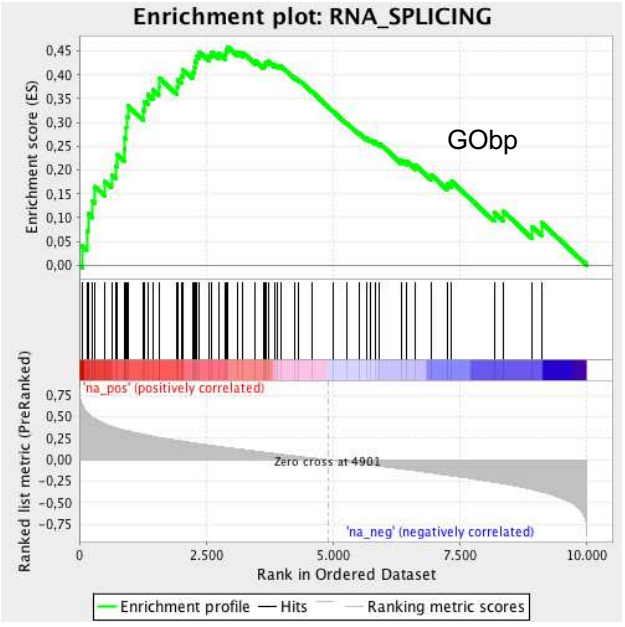

D

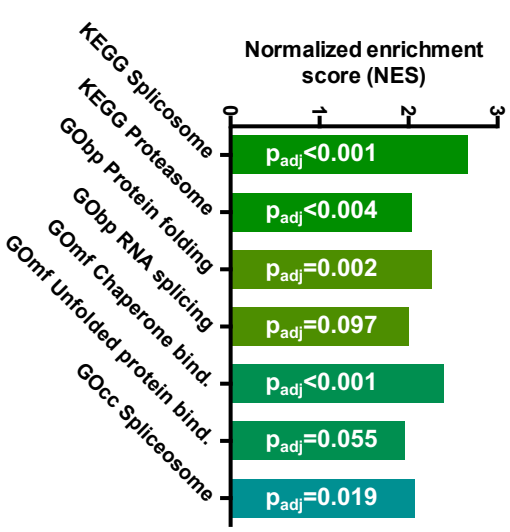

E